



Free Vibration Analysis of Advanced Composite Plates with Porosities

S. Merdaci^{1*}, H. Belghoul², A. Hadj Mostefa³, M. Merazi, H. Hellal⁴, S. Boutaleb⁴

¹*Structures and Advanced Materials in Civil Engineering and Public Works Laboratory, University of Sidi Bel Abbes, Faculty of Technology, Civil Engineering and Public Works Department, Algeria.*

²*Laboratory of Mechanics Physics of Materials (LMPM), University of Djillali Liabès of Sidi Bel Abbes, Algeria.*

³*Laboratory of Industrial Engineering and Sustainable Development, Department Civil Engineering, Institute of Science & Technology, University of Rélizane, Algeria.*

⁴*Laboratory of Materials and Hydrology, University of Sidi Bel Abbes, Faculty of Technology, Department of Civil Engineering and Public Works, BP 89 Cité Ben M'hidi, 22000 Sidi Bel Abbes, Algeria.*

* Corresponding author. Dr S. Merdaci email: slimanem2016@gmail.com

Abstract. This article presents the free vibration analysis of advanced composite plates such as functionally graded plates and of simply supported plate porous using a high order shear deformation theory. In is work the material properties of the porous plate FG vary across the thickness. The proposed theory contains four unknowns unlike the other theories. Therefore, it is useless to use the shear correction factors. The Hamilton's principle will be used herein to determine the equations of motion. Since, the plate are simply supported the Navier procedure will be retained. To show the precision of this model, several comparisons have been made between the present results and those of existing theories in the literature for non-porous plates. Effects of the exponent graded and porosity factors are investigated.

Keywords. Composite plates, FG, high order theory, Hamilton's principle, free vibration; porosity.

INTRODUCTION

Functionally graded materials (FGMs) are a class of advanced composite materials. The mechanical properties of FGMs change continuously over the thickness of structures. In general, FGM is made from a mixture of ceramic and metal. In recent years, they have gained significant attention in many engineering fields such as automotive, civil engineering, aerospace, and nuclear engineering. Hence, due to the exotic properties of FGMs, many researchers have been captivated to investigate the bending behaviors, free vibration, and dynamic and buckling behaviors of FGM beams, plates, and shells. According to the literature, the analysis of FGM plates can be investigated with some different theories such as the classical

plate theory (CPT), the first-order shear deformation theory (FSDT) and higher-order shear deformation theory (HSDT). To remedy such defects, functionally graded materials (FGMs), within which material properties vary continuously, have been proposed.

The concept of FGM was proposed in 1984 by a group of materials scientists, in Sendai, Japan, for thermal barriers or heat shielding properties.

In recent years, extensive studies relevant to FG plates are carried out by using the classical plate theory (CPT) and first-order shear-deformation plate theory (FSDT). Despite the simplicity of the CPT (or the Kirchhoff–Love theory), the CPT disregards shear deformations and rotary inertia, resulting in unreliable results for thick and moderately thick plates. The FSDT (or Reissner–Mindlin plate theory) supports transverse shear effects by using a shear correction factor and hence is appropriate for analysis of both moderately thick and thin plates. However, the suitable value of the shear correction factor depends on the variation of Poisson’s ratio through the thickness of the plate, geometry, loading and boundary conditions. The higher-order-shear-deformation theories (HSDTs) do not need a shear correction factor and provide the best accuracy compared with CPT and FSDT.

It is grasped that in the process of FGM manufacturing, micro voids (known as porosities) can take place within the materials during the sintering action (Zhu, 2001; Li, 2003). This phenomenon is related to the large difference in solidification temperatures between material components (Zhu, 2001; Wang, 2017). Due to the importance of this subject, several studies have been carried out to explore the porosity effects. For example, Yahia (2015) studied the wave distribution of FG plates with porosities by utilizing various R-HSDTs with application in ultrasonic inspection techniques. A higher order shear deformation theory was used for the study on free vibration of micro beams made of porous graded materials by (Atmane, 2015). (Gupta and Talha, 2017) examined the effect of porosity on the frequency response of FG plates in the presence of a thermal effect by using a non-polynomial higher-order shear and normal deformation theory.

However, in the manufacture of FGMs, micro-porosities or voids can occur in the materials during the sintering process. This is due to the large difference in solidification temperature between the material constituents (Zhu, 2001). Wattanasakulpong (2012) also gave a discussion of the porosities that occur within FGM specimens made by a sequential multi-step infiltration technique. Therefore, it is important to take into account the effect of porosity in the design of FGM structures subjected to static (Merdaci, 2018; 2019) and dynamic loads (Wattanasakulpong, 2014; Merdaci, 2019). Consequently, studies devoted to understanding the static and dynamic behavior of FGM material structures have been given more and more attention in recent years.

This work aims at developing a new simple theory of high order shear deformation for the analysis of the free vibration of advanced composite plates, such as FGM plates by considering the porosities that can occur inside the materials with gradient properties (FG) at during their manufacture. The proposed theory contains four unknowns unlike the other theories, which contain five known at most, this theory it checks the boundary conditions without constraints on the upper and lower surfaces of the plate without the aid of shear correction factor. Analytical solutions are obtained for the FG pallet by the present theory and its accuracy is verified by comparing the results obtained with those reported in the literature. The effects of various parameters, such as thickness ratio and volume fraction of porosity on the free vibration of FG plates are all discussed.

MATERIALS AND METHODS

Material properties and mathematical model of advanced composite plates

Advanced composite materials such as functionally graded materials can be produced by continuously varying the constituents of multi-phase materials in a predetermined profile. An FGM can be defined by the variation in the volume fractions (Fig.1). The material properties of the plate FG, such as Young's modulus E , are assumed function of the volume fraction of constituent materials. The properties of the FGM vary continuously due to the progressive volume fraction of the constituents of the materials (ceramic and metal), generally in the direction of the thickness. In this paper, FGM plates with the power-law function (P-FGM) were considered (Fig.2).

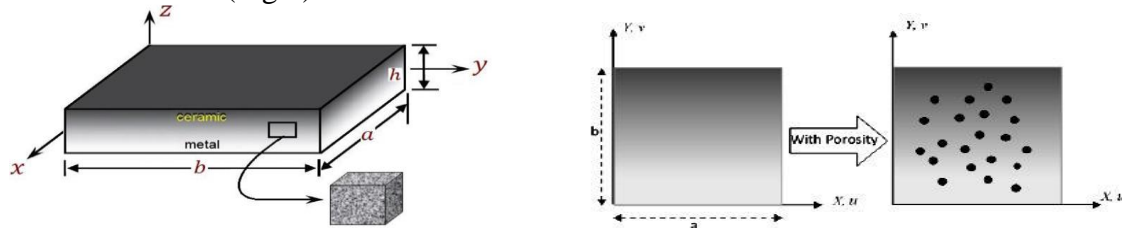


Fig. 1. Geometric configuration of plate FG with porosity.

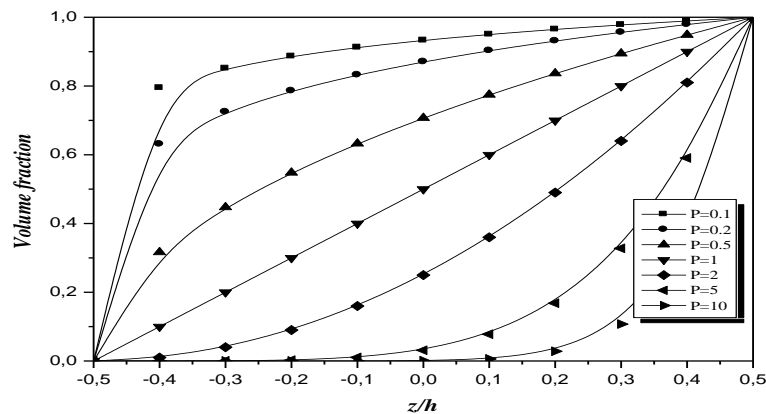


Fig. 2. Variation of the volume fraction across the thickness of a plate.

For the case of P-FGM plates, the materials properties of P-FGM depend on the volume fraction, which can be obtained as a power-law function as the following formula. Consider an imperfect FG with a volume fraction of porosity, ξ , ($0 \leq \xi \leq 1$) distributed uniformly between metal and ceramic, the law of the modified mixture proposed by (Wattanasakulpong and Ungbhakorn, 2014) is used as:

$$E(z) = E_m \left(1 - V - \frac{\xi}{2} \right) + E_c \left(V - \frac{\xi}{2} \right) \quad (1a)$$

$$\rho(z) = \rho_m \left(1 - V - \frac{\xi}{2} \right) + \rho_c \left(V - \frac{\xi}{2} \right) \quad (1b)$$

$$V = \left(\frac{1}{2} - \frac{z}{h} \right)^P \quad (1c)$$

Where: E_c and E_m are the corresponding properties of the ceramic and metal,

“ ρ ” density of material, respectively,

“ P ” is the volume fraction exponent, which takes values greater than or equal to zero.

The above power-law assumption reflects a simple rule of mixtures used to obtain the effective properties of the ceramic-metal plate. The rule of mixtures applies only to the thickness

direction. Note that the volume fraction of the metal is high near the bottom surface of the plate, and that of the ceramic is high near the top surface.

Formulation of high order shear deformation theory

Kinematics and constitutive equations

Corresponding to the simple HSDT, the transverse displacement w is separated into two parts the bending constituent w_b and the shear constituent w_s . In the present analysis, the shear deformation plate theory is suitable for the displacements (Merdaci, 2011):

$$\begin{aligned} u(x, y, z) &= u_0(x, y) - z \frac{\partial w_b}{\partial x} + \left(\frac{z}{2} \left(\frac{h^2}{4} - \frac{z^2}{3} \right) \right) \frac{\partial w_s}{\partial x} \\ v(x, y, z) &= v_0(x, y) - z \frac{\partial w_b}{\partial y} + \left(\frac{z}{2} \left(\frac{h^2}{4} - \frac{z^2}{3} \right) \right) \frac{\partial w_s}{\partial y} \\ w(x, y, z) &= w_b(x, y) + w_s(x, y) \end{aligned} \quad (2a)$$

The strains associated with the displacements in equation 5 are:

$$\begin{aligned} \begin{Bmatrix} \varepsilon_x \\ \varepsilon_y \\ \gamma_{xy} \\ \gamma_{yz} \\ \gamma_{xz} \end{Bmatrix} &= \begin{Bmatrix} \varepsilon_x^0 + z k_x^b + f(z) k_x^s \\ \varepsilon_y^0 + z k_y^b + f(z) k_y^s \\ \gamma_{xy}^0 + z k_{xy}^b + f(z) k_{xy}^s \\ f'(z) \gamma_{yz}^s \\ f'(z) \gamma_{xz}^s \end{Bmatrix} \quad (2b) \\ \begin{Bmatrix} \varepsilon_x^0 \\ \varepsilon_y^0 \\ \gamma_{xy}^0 \end{Bmatrix} &= \begin{Bmatrix} \frac{\partial u_0}{\partial x} \\ \frac{\partial v_0}{\partial y} \\ \frac{\partial u_0}{\partial y} + \frac{\partial v_0}{\partial x} \end{Bmatrix}, \quad \begin{Bmatrix} k_x^b \\ k_y^b \\ k_{xy}^b \end{Bmatrix} = \begin{Bmatrix} -\frac{\partial^2 w_b}{\partial x^2} \\ -\frac{\partial^2 w_b}{\partial y^2} \\ -2 \frac{\partial^2 w_b}{\partial x \partial y} \end{Bmatrix}, \quad \begin{Bmatrix} k_x^s \\ k_y^s \\ k_{xy}^s \end{Bmatrix} = \begin{Bmatrix} \frac{\partial^2 w_s}{\partial x^2} \\ \frac{\partial^2 w_s}{\partial y^2} \\ 2 \frac{\partial^2 w_s}{\partial x \partial y} \end{Bmatrix}, \quad \begin{Bmatrix} \gamma_{yz}^s \\ \gamma_{xz}^s \end{Bmatrix} = \begin{Bmatrix} \frac{\partial w_s}{\partial y} \\ \frac{\partial w_s}{\partial x} \end{Bmatrix}, \quad (2c) \end{aligned}$$

$$g(z) = 1 - f'(z), \quad f'(z) = \frac{df(z)}{dz} \quad (2d)$$

The stress-strain relations for a linear elastic plate and isotropic, are written in the following:

$$\begin{Bmatrix} \sigma_{xx} \\ \sigma_{yy} \\ \tau_{xy} \\ \tau_{yz} \\ \tau_{xz} \end{Bmatrix} = \begin{bmatrix} Q_{11} & Q_{12} & 0 & 0 & 0 \\ Q_{21} & Q_{22} & 0 & 0 & 0 \\ 0 & 0 & Q_{66} & 0 & 0 \\ 0 & 0 & 0 & Q_{44} & 0 \\ 0 & 0 & 0 & 0 & Q_{55} \end{bmatrix} \begin{Bmatrix} \varepsilon_{xx} \\ \varepsilon_{yy} \\ \gamma_{xy} \\ \gamma_{yz} \\ \gamma_{xz} \end{Bmatrix} \quad (2f)$$

Where: $(\sigma_x, \sigma_y, \tau_{xy}, \tau_{yz}, \tau_{yx})$ and $(\varepsilon_x, \varepsilon_y, \gamma_{xy}, \gamma_{yz}, \gamma_{yx})$ are the stress and strain components, respectively.

Using the material properties defined in equation (2g), the stiffness coefficients, Q_{ij} , can be expressed as:

$$Q_{11} = Q_{22} = \frac{E(z)}{1-\nu^2}, \quad Q_{12} = \frac{\nu E(z)}{1-\nu^2}, \quad Q_{44} = Q_{55} = Q_{66} = \frac{E(z)}{2(1+\nu)}, \quad (2g)$$

Equations of motion

The equations of motion can be quantified using the Hamilton's principle that is:

$$\int_0^T (\delta U - \delta K) dt = 0 \quad (3a)$$

Where: δU : variation of strain energy; δK : variation of kinetic energy.

The variation of strain energy of the plate is calculated by:

$$\delta U = \int_{-h/2}^{h/2} \int_A [\sigma_x \delta \varepsilon_x + \sigma_y \delta \varepsilon_y + \tau_{xy} \delta \gamma_{xy} + \tau_{yz} \delta \gamma_{yz} + \tau_{xz} \delta \gamma_{xz}] dA dz \quad (3b)$$

Where A is the top surface, and stress resultants N, M, and S are defined by:

$$\begin{Bmatrix} N_x & N_y & N_{xy} \\ M_x^b & M_y^b & M_{xy}^b \\ M_x^s & M_y^s & M_{xy}^s \end{Bmatrix} = \int_{-h/2}^{h/2} (\sigma_x, \sigma_y, \tau_{xy}) \begin{Bmatrix} 1 \\ z \\ f(z) \end{Bmatrix} dz, \quad (S_{xz}^s, S_{yz}^s) = \int_{-h/2}^{h/2} (\tau_{xz}, \tau_{yz}) g(z) dz. \quad (3c)$$

The variation of kinetic energy of the plate can be written as:

$$\delta K = \int_{-h/2}^{h/2} \int_A \rho(z) (\dot{u} \delta u + \dot{v} \delta v + \dot{w} \delta w) dA dz \quad (3d)$$

Where dot-superscript convention indicates the differentiation with respect to the time variable t.

($I_1, I_2, I_3, I_4, I_5, I_6$) are mass inertias defined as:

$$(I_1, I_2, I_3, I_4, I_5, I_6) = \int_{-h/2}^{h/2} (1, z, z^2, f(z), zf(z), f(z)^2) \rho(z) dz \quad (3e)$$

Substituting the expressions for δU and δK from equations (3b) and (3d) into equation (3a), integrating the displacement gradients by parts and setting the coefficients δu , δv , δw_b , and δw_s zero separately.

Thus, one can obtain the equilibrium equations associated with the present shear deformation theory,

$$\begin{aligned} \delta u : \quad \frac{\partial N_x}{\partial x} + \frac{\partial N_{xy}}{\partial y} &= I_1 \dot{u}_0 - I_2 \frac{\partial \dot{w}_b}{\partial x} - I_4 \frac{\partial \dot{w}_s}{\partial x} \\ \delta v : \quad \frac{\partial N_{xy}}{\partial x} + \frac{\partial N_y}{\partial y} &= I_1 \dot{v}_0 - I_2 \frac{\partial \dot{w}_b}{\partial y} - I_4 \frac{\partial \dot{w}_s}{\partial y} \\ \delta w_b : \quad \frac{\partial^2 M_x^b}{\partial x^2} + 2 \frac{\partial^2 M_{xy}^b}{\partial x \partial y} + \frac{\partial^2 M_y^b}{\partial y^2} &= I_1 (\dot{w}_b + \dot{w}_s) + I_2 \left(\frac{\partial \dot{u}}{\partial x} + \frac{\partial \dot{v}}{\partial y} \right) - I_3 \left(\frac{\partial^2 \dot{w}_b}{\partial x^2} + \frac{\partial^2 \dot{w}_b}{\partial y^2} \right) - I_5 \left(\frac{\partial^2 \dot{w}_s}{\partial x^2} + \frac{\partial^2 \dot{w}_s}{\partial y^2} \right) \\ \delta w_s : \quad \frac{\partial^2 M_x^s}{\partial x^2} + 2 \frac{\partial^2 M_{xy}^s}{\partial x \partial y} + \frac{\partial^2 M_y^s}{\partial y^2} + \frac{\partial S_{xz}^s}{\partial x} + \frac{\partial S_{yz}^s}{\partial y} &= I_1 (\dot{w}_b + \dot{w}_s) + I_4 \left(\frac{\partial \dot{u}}{\partial x} + \frac{\partial \dot{v}}{\partial y} \right) - I_5 \left(\frac{\partial^2 \dot{w}_b}{\partial x^2} + \frac{\partial^2 \dot{w}_b}{\partial y^2} \right) - I_6 \left(\frac{\partial^2 \dot{w}_s}{\partial x^2} + \frac{\partial^2 \dot{w}_s}{\partial y^2} \right) \end{aligned} \quad (3f)$$

Analytical solutions for FG plates

Rectangular plates are generally classified according to the type of support used. This paper is concerned with the exact solution for a simply supported FG plate. The following boundary conditions are imposed at the side edges:

$$v_0 = w_b = w_s = \frac{\partial w_b}{\partial y} = \frac{\partial w_s}{\partial y} = N_x = M_x^b = M_x^s = 0 \quad \text{and} \quad x=0, a \quad (4a)$$

$$u_0 = w_b = w_s = \frac{\partial w_b}{\partial x} = \frac{\partial w_s}{\partial x} = 0, N_y = M_y^b = M_y^s = 0 \quad \text{and} \quad y=0, b \quad (4b)$$

Following the Navier solution procedure, we assume the following form of solution for (u, v, w_b, w_s) that satisfies the boundary conditions given in equation (4c).

$$\begin{cases} u \\ v \\ w_b \\ w_s \end{cases} = \sum_{m=1}^{\infty} \sum_{n=1}^{\infty} \begin{cases} U_{mn} e^{i\omega t} \cos(\lambda x) \sin(\mu y) \\ V_{mn} e^{i\omega t} \sin(\lambda x) \cos(\mu y) \\ W_{bmn} e^{i\omega t} \sin(\lambda x) \sin(\mu y) \\ W_{smn} e^{i\omega t} \sin(\lambda x) \sin(\mu y) \end{cases}, \quad (4c)$$

Where: U_{mn}, V_{mn}, W_{bmn} , and W_{smn} are arbitrary parameters can be combined into a system of equations as: $([K] - \omega^2 [M])\{\Delta\} = \{0\}$, (4d)

Where: $[K]$ and $[M]$, stiffness and mass matrices, respectively, and represented as:

$$[K] = \begin{bmatrix} a_{11} & a_{12} & a_{13} & a_{14} \\ a_{12} & a_{22} & a_{23} & a_{24} \\ a_{13} & a_{23} & a_{33} & a_{34} \\ a_{14} & a_{24} & a_{34} & a_{44} \end{bmatrix},$$

$$[K] = \begin{bmatrix} -I_1 & 0 & \lambda I_2 & \lambda I_4 \\ 0 & -I_1 & \mu I_2 & \mu I_4 \\ \lambda I_2 & \mu I_2 & -I_1 - I_3(\lambda^2 + \mu^2) & -I_5(\lambda^2 + \mu^2) \\ \lambda I_4 & \mu I_4 & -I_5(\lambda^2 + \mu^2) & -I_6(\lambda^2 + \mu^2) \end{bmatrix} \quad (4e)$$

$$\{\Delta\}^T = \{U_{mn}, V_{mn}, W_{bmn}, W_{smn}\}, \quad (4f)$$

Where: $\lambda = m\pi/a$ and $\mu = n\pi/b$, « m » and « n » are mode numbers.

$$\begin{aligned} a_{11} &= -(A_{11}\lambda^2 + A_{66}\mu^2); a_{12} = -\lambda \mu (A_{12} + A_{66}); a_{13} = \lambda [B_{11}\lambda^2 + (B_{12} + 2B_{66})\mu^2]; a_{14} = \lambda [B_{11}^s\lambda^2 + (B_{12}^s + 2B_{66}^s)\mu^2] \\ a_{21} &= a_{12}; a_{22} = -(A_{66}\lambda^2 + A_{22}\mu^2); a_{23} = \mu [(B_{12} + 2B_{66})\lambda^2 + B_{22}\mu^2]; a_{24} = \mu [(B_{12}^s + 2B_{66}^s)\lambda^2 + B_{22}^s\mu^2] \\ a_{31} &= a_{13}; a_{32} = a_{23}; a_{33} = -(D_{11}\lambda^4 + 2(D_{12} + 2D_{66})\lambda^2\mu^2 + D_{22}\mu^4); a_{34} = -(D_{11}^s\lambda^4 + 2(D_{12}^s + 2D_{66}^s)\lambda^2\mu^2 + D_{22}^s\mu^4) \\ a_{41} &= a_{14}; a_{42} = a_{24}; a_{43} = a_{34}; a_{44} = -(H_{11}^s\lambda^4 + 2(H_{12}^s + 2H_{66}^s)\lambda^2\mu^2 + H_{22}^s\mu^4 + A_{55}^s\lambda^2 + A_{44}^s\mu^2) \end{aligned} \quad (4f)$$

RESULTS AND DISCUSSION

In this section, various numerical examples are presented and discussed to verify the accuracy of the present theory in predicting the free vibration responses of simply supported FG plates. One type of FG plates of Al/ZrO₂ are used in this study. The material properties of FG plates are:

- Metal (Aluminum (Al)): $E_m = 70$ GPa; $\nu = 0.3$; $\rho = 2702$ kg/m³.
- Ceramic (Zirconia (ZrO₂)): $E_c = 211$ GPa; $\nu = 0.3$; $\rho = 4500$ kg/m³.

The different modes of displacement are presented (CPT: Classical plate theory, FSDPT: First-order shear deformation theory, HSDPT: Higher-order shear deformation plate theory); a comparison with the numerical case studies is used to check the accuracy of the present analysis. Unless otherwise has been stated, the following relations have been used for presentations of non-dimensional natural frequencies. The material properties of the plate FG are supposed to vary according to the thickness of the plate according to a simple law of power P-FGM. The lower part of the FG plate is rich in Metal (Aluminum, Al), while the upper surface is rich in ceramics (Zirconia, ZrO₂). For convenience, the non-dimensional parameter used in this study is:

$$\hat{\omega} = \omega h \sqrt{\frac{\rho}{G}}, \quad \varpi = \left(\frac{a^2}{h}\right) \sqrt{\frac{\rho_c}{E_c}} \quad (5)$$

The non-dimensionalized natural frequencies of general rectangular isotropic and FG Al/ZrO₂ plates are considered for comparison. In table.1 compares natural frequencies obtained by the

present theory for a thick square isotropic plate with those given by (Reddy and Phan, 1985) based on HSDPT (Reddy and Phan, 1985) , by (Whitney and Pagano, 1970) based on first shear deformation theory FSDPT and well-known (Love–Kirchhoff, 1950) plate theory or (CPT) in which the transverse shear strain is neglected. Comparison of results shows that the present theory, which takes into account both the transverse shear and transverse normal deformation, predicts the natural frequencies with the same degree of accuracy as that of solutions at lower as well as higher modes. However, the three other theories (Love–Kirchhoff, 1950; Reddy and Phan, 1985; Whitney and Pagano, 1970), which neglect the thickness stretching effect ($\epsilon z = 0$), slightly underestimate frequency compared to the present theory.

Table 1. Non-dimensional natural frequencies $\hat{\omega}$ for simply supported isotropic square plate ($a/b=1$, $a/h=10$) and the porosity coefficients $\xi=0$.

m	n	CPT	FSDPT	HSDPT	Present
1	1	0.0955	0.0930	0.0931	0.0930
1	2	0.2360	0.2219	0.2222	0.2220
2	2	0.3732	0.3406	0.3411	0.3406
1	3	0.4629	0.4149	0.4158	0.4151
2	3	0.595 1	0.5206	0.5221	0.5208
3	3	0.8090	0.6834	0.6862	0.6840
2	4	0.8926	0.7446	0.7481	0.7454
1	5	1.1365	0.9174	0.9230	0.9187
4	4	1.3716	1.0764	1.0847	1.0785

It can be concluded that the present theory is not only accurate but also efficient and simple in predicting the free vibration responses of plates FG non-porous ($\xi=0.0$).

From the curves presented in figure 3, it can be noted that more than the parameter of the power index of the material "P" is high, more than the fundamental frequency in the porous ($\xi=0.1$ and 0.2) and non-porous($\xi=0.0$) plate FG structures is decreased, which whatever the number of waves. However, increasing the porosity factor causes an increase in the frequency. Therefore, the maximum frequency is obtained for a ceramic plate ($P = 0$).

The non-dimensional fundamental natural frequency ν of simply supported rectangular FG plates ($b=2a$) and power law index P for various values of side-to-thickness ratios (a/h) and different porosity factor ($\xi = 0.0 ; 0.10$ and 0.20) are plotted in figure 4 based on the present high order shear deformation theory. As shown, the frequency decreases significantly with the increase of P. It is, basically, attributable to the fact that Young's modulus of ceramic is higher than metal. The variation of frequency parameter with aspect ratios (b/a) of FG plates using the present theory is plotted in figure 5.

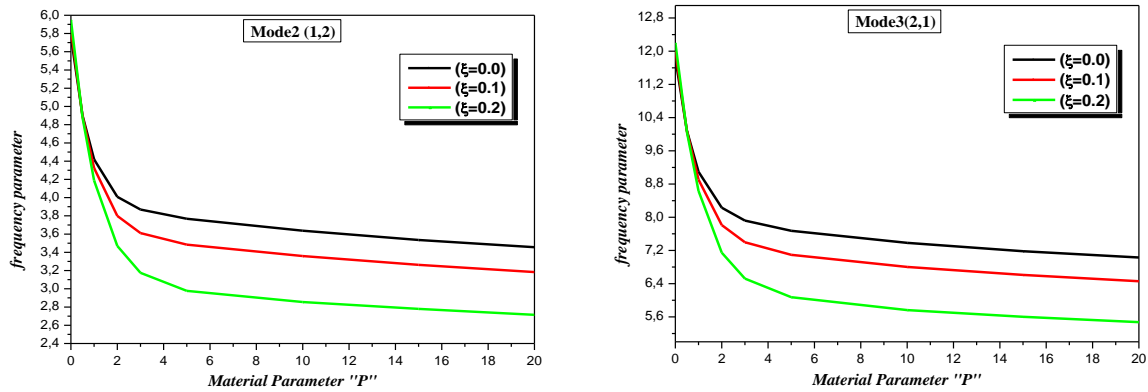


Fig. 3. Variation of the fundamental frequency $\bar{\omega}$ of plate FG porous according to the material power index "P".

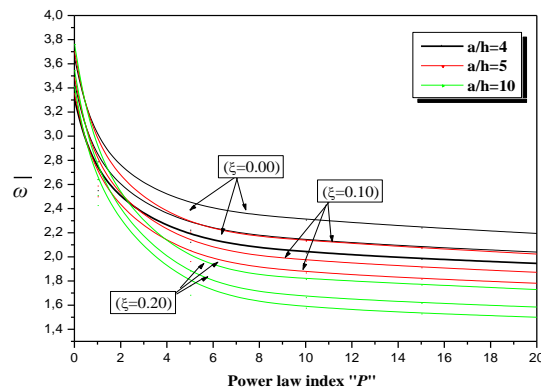


Fig. 4. Fundamental natural frequency $\bar{\omega}$ of simply supported FG rectangular plates ($b=2a$) as function of power law index "P" for different porosity factor (ξ).

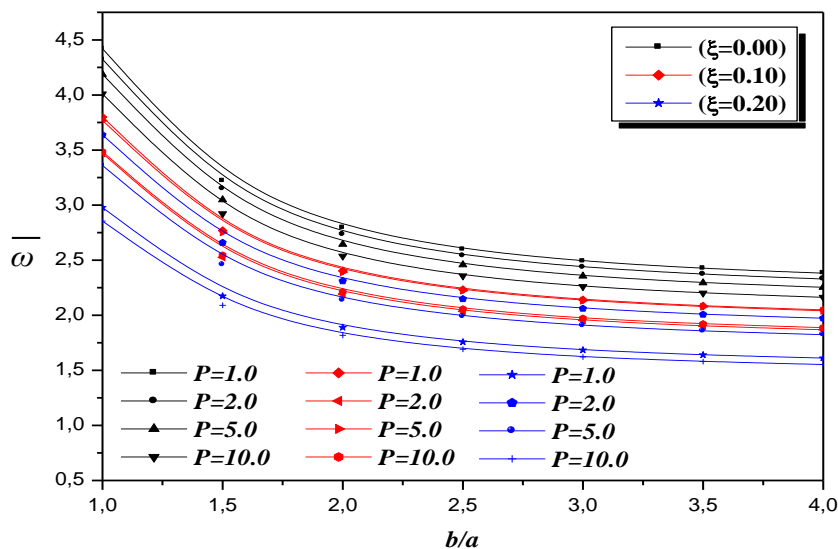


Fig. 5. Natural frequency of simply supported FG plates ($a/h=10$) as function of aspect ratio (b/a) for different power law index "P" and different porosity factor (ξ).

CONCLUSION

In this work, the analysis of the free vibration of advanced composite plates such as functionally graded plates with porosities is examined by a new simple theory of high order shear deformation. Herein, a summary of most significant results is presented as follows:

- This theory satisfies the nullity of the stresses at the upper and lower surfaces of the plate without using the shear correction factor.
- The law of the modified mixture covering the porosity phases is used to roughly describe the properties of plate FG with porosity.
- The equations of motion are derived from the principle of virtual works and the principle of Hamilton.
- The effects of various parameters, such as the thickness ratio and the volume fraction of the porosity on the free vibration of FG plates are all discussed.
- The present theory gave control results that can be used to evaluate various plate theories, and to compare with the results obtained by another (Love–Kirchhoff, 1950; Reddy and Phan, 1985 and Whitney and Pagano, 1970).
- The present theory of plate FG proposed is accurate and simple for the resolution of the mechanical behavior of FG plates with porosity.

REFERENCES

- Atmane H.A., Tounsi A., Bernard F., Mahmoud S., 2015. *Steel Compos. Struct.* 19, 369–384.
- Gupta A., Talha M., 2017. *Int. J. Struct. Stab. Dyn.* 1850013.
- Hadj Mostefa A., Merdaci S., Mahmoudi N., 2018. *Proceedings of the Third International Symposium on Materials and Sustainable Development*, ISBN 978-3-319-89706-6, 267–278.
- Jha D.K., Kant T., Singh R.K., 2012. *Nucl. Eng. Des.* 250, 8–13.
- Kirchhoff G., *Journal fur reine und angewandte Mathematik.* 40, 51-88.
- Li J.F., Takagi K., Ono M., Pan W., Watanabe R., Almajid A., Taya M., 2003. *J. Am. Ceram. Soc.* 86, 1094–1098.
- Merdaci S., Tounsi A., Houari M.S.A., Mechab I., Hebali H., Benyoucef S., 2011. *Arch. Appl. Mech.* 81 1507e22.
- Merdaci S., Tounsi A., Bakora A., 2016. *An International Journal Steel & Composite Structures.* 22(4), 713-732.
- Merdaci S., 2017. *International Journal of Engineering Research And Advanced Technology (IJERAT).* 3 (8), 49-59.
- Merdaci S., 2018. *Advanced Engineering Forum.* 30, 54-70.
- Merdaci S., 2018. *Algerian Journal of Research and Technology.* 2 (1), 54-69.
- Merdaci S., Belghoul H., 2019. *Comptes rendus Mecanique.* 347(3), 207-217.
- Merdaci S., 2019. *Nano Hybrids and Composites.* 25, 69-83.
- Reddy J. N., 1984. *J. Appl. Mech.* 51(4), 745.
- Reddy J. N., 2000. *Int. J. Numer. Methods Eng.* 47, 663–684. 404.
- Reddy J. N., 2002. Wiley, New York, 406.
- Reddy J. N., Phan N. D., 1985. *J. Sound Vibrat.* 98, 157–170.
- Shahrjerdi A., Mustapha F., Bayat M., Sapuan S. M., Zahari R., Shahzamanian M. M., 2011. *Mater. Sci. Eng.* 17,10.1088/1757- 412 899X/17/1/012008.
- Wang Y.Q., Zu J.W., 2017. *Aerosp. Sci. Tech- nol.*
- Wattanasakulpong N., Prusty B.G., Kelly D.W., Hoffman M., 2012. *Mater. Des.* 36, 182-190.
- Wattanasakulpong N., Ungbhakorn V., 2014. *Aerosp.Sci. Technol.* 32(1), 111-120.
- Yahia S.A., Atmane H.A., Houari M.S.A., Tounsi A., 2015. *Struct. Eng. Mech.* 53, 1143–1165.
- Zhu J., Lai Z., Yin Z., Jeon J., Lee S., 2001. *Mater. Chem. Phys.* 68, 130–135.

Zhu J., Lai Z., Yin Z., Jeon J., Lee, S., 2001. Mater. Chem. Phys. 68(1-3), 130-135.
Whitney J. M., Pagano N. J., 1970. J. Appl. Mech. 37, 1031–1036.